

# Sorbitol Crystallization-Induced Aggregation in Frozen mAb Formulations

DEIRDRE MURPHY PIEDMONTE,<sup>1</sup> ALISON HAIR,<sup>1</sup> PRITI BAKER,<sup>1,2</sup> LEJLA BRYCH,<sup>1</sup> KARTHIK NAGAPUDI,<sup>1,3</sup> HONG LIN,<sup>1,3</sup> WENJIN CAO,<sup>1</sup> SUSAN HERSHENSON,<sup>1,4</sup> GAYATHRI RATNASWAMY<sup>1,5</sup>

<sup>1</sup>Amgen Inc., One Amgen Center Dr., Thousand Oaks, California 91320

<sup>2</sup>Priti Baker's present address is Biogen Idec, Research Triangle Park, North Carolina 27709

<sup>3</sup>Hong Lin's present address is Genentech Inc., South San Francisco, California 94080

<sup>4</sup>Susan Hershenson's present address is Bill and Melinda Gates Foundation, Seattle, Washington 98109

<sup>5</sup>Gayathri Ratnaswamy's present address is Agensys Inc., Santa Monica, California 90404

Received 10 June 2014; revised 31 July 2014; accepted 6 August 2014

Published online 12 September 2014 in Wiley Online Library (wileyonlinelibrary.com). DOI 10.1002/jps.24141

**ABSTRACT:** Sorbitol crystallization-induced aggregation of mAbs in the frozen state was evaluated. The effect of protein aggregation resulting from sorbitol crystallization was measured as a function of formulation variables such as protein concentration and pH. Long-term studies were performed on both IgG1 and IgG2 mAbs over the protein concentration range of 0.1–120 mg/mL. Protein aggregation was measured by size-exclusion HPLC (SE-HPLC) and further characterized by capillary-electrophoresis SDS. Sorbitol crystallization was monitored and characterized by subambient differential scanning calorimetry and X-ray diffraction. Aggregation due to sorbitol crystallization is inversely proportional to both protein concentration and formulation pH. At high protein concentrations, sorbitol crystallization was suppressed, and minimal aggregation by SE-HPLC resulted, presumably because of self-stabilization of the mAbs. The glass transition temperature ( $T_g'$ ) and fragility index measurements were made to assess the influence of molecular mobility on the crystallization of sorbitol.  $T_g'$  increased with increasing protein concentration for both mAbs. The fragility index decreased with increasing protein concentration, suggesting that it is increasingly difficult for sorbitol to crystallize at high protein concentrations. © 2014 Wiley Periodicals, Inc. and the American Pharmacists Association *J Pharm Sci* 104:686–697, 2015

**Keywords:** protein formulation; excipients; crystallization; calorimetry (DSC); glass transition temperature; stabilization; X-ray diffraction; protein aggregation; HPLC; mAb

## INTRODUCTION

A strategy commonly used in the biopharmaceutical industry to extend the shelf life of mAb formulations is to freeze process intermediates such as drug substance. Although the frozen state can afford improved stability, it is well documented that freezing can subject proteins to several potentially destabilizing stresses: protein exposure to the ice surface, high concentrations of solutes in the freeze concentrate, changes in the pH of the freeze concentrate (due to the crystallization of buffer salts that become concentrated upon freezing, thereby exceeding their solubility), and cold denaturation.<sup>1–4</sup> Presumably, colder temperatures (ca.  $-80^{\circ}\text{C}$ ) afford improved long-term stability because of reduced molecular mobility in the frozen state. Because limited molecular mobility can translate into decreased rates of chemical and physical degradation, ideally samples should be stored in the glassy state (below the  $T_g'$ ). However, practical requirements often necessitate that process intermediates are stored in warmer, walk-in freezers.

Excipients are used to stabilize a protein in the frozen state by mitigating the aforementioned stresses. However, for an excipient to stabilize a protein during freezing and throughout

frozen storage, the excipient must remain in the same amorphous phase as the protein.<sup>5,6</sup> It is important to understand the phase transitions that an excipient may undergo during frozen storage in order to ensure adequate protein stability. Moreover, monitoring for excipient phase transitions during freeze drying is important to ensure protein stability, as was reported by Sundaramurthi et al.<sup>7</sup> who discovered the crystallization of trehalose during the annealing step of lyophilization. Parameters critical to effectively stabilize proteins in the frozen state include protein concentration and recommended storage temperature, which can be influenced by other factors such as dosing regimen and large-scale freezer availability, respectively.

The excipient sorbitol affords long-term stability at  $2^{\circ}\text{C}$ – $8^{\circ}\text{C}$  and is commonly used to stabilize liquid parenteral formulations, such as Neupogen® (filgrastim)<sup>8</sup> and Neulasta® (pegfilgrastim).<sup>9</sup> Although sorbitol was considered an amorphous excipient in the frozen state,<sup>10,11</sup> we previously reported that a sorbitol-containing formulation (2 mg/mL N-terminal Fc (fragment, crystallizes easily) fusion protein) crystallized upon long-term storage at  $-30^{\circ}\text{C}$ . Upon crystallization, sorbitol undergoes phase separation from the protein, which ultimately induces protein aggregation.<sup>12</sup>

Building upon our previous work, here we assessed sorbitol crystallization-induced aggregation in mAbs primarily as a function of protein concentration (from 0.1 to 120 mg/mL). We also monitored the effect of pH on sorbitol crystallization and consequent protein aggregation. The covalent character of the resulting aggregate was also assessed. The role of molecular

**Abbreviations used:** SE-HPLC, size-exclusion HPLC; CE-SDS, capillary-electrophoresis SDS; DSC, differential scanning calorimetry;  $T_g'$ , glass transition temperature; XRD, X-ray diffraction.

**Correspondence to:** Deirdre Murphy Piedmonte (Telephone: +805-313-6503; Fax: +805-447-3401; E-mail: deirdrem@amgen.com)

*Journal of Pharmaceutical Sciences*, Vol. 104, 686–697 (2015)

© 2014 Wiley Periodicals, Inc. and the American Pharmacists Association

mobility in the propensity of sorbitol formulations to crystallize was explored by measuring the glass transition temperatures of sorbitol-containing formulations over a 1000-fold range of protein concentration. In addition to routine  $T_g'$  measurements, measuring fragility index by differential scanning calorimetry (DSC) has been used to understand dynamics in the supercooled liquid.<sup>13–15</sup> Approaching the glass transition from the liquid side, it has been observed that supercooled liquids differ in the rate of change of viscosity with temperature. This difference in rate of change of viscosity among supercooled liquids as a function of temperature is related to differences in dynamic heterogeneity. This observation has led to the classification of supercooled fluids in terms of their fragility as “kinetic fragility.”<sup>16</sup> When approaching the glass transition, fragile liquids show a faster change in viscosity with temperature than strong liquids. Correlations between fragility and other glass properties have been sought and tested over the years to better understand the glassy state.<sup>17–20</sup> In this paper, we report fragility index measurements of sorbitol-containing formulations over a broad concentration range. Such measurements can improve our understanding of the dynamic heterogeneity of systems with different protein concentrations and can also shed light on the potential for identifying formulation conditions where sorbitol crystallization may occur. The goal of this work was to understand sorbitol crystallization-induced aggregation, which may then provide the flexibility to freeze process intermediates of sorbitol-containing formulations.

## MATERIALS AND METHODS

### Sample Preparation and Storage

The IgG1 and IgG2 molecules were expressed in mammalian cells and purified at Amgen Inc. (Thousand Oaks, California). In studies performed with the IgG1 molecule, a 70 mg/mL protein solution was diluted with formulation buffer (10 mM acetate at pH 5.2 with 274 mM sorbitol) to the desired protein concentrations. Protein concentrations were verified by UV–vis spectroscopy at 280 nm using the appropriate extinction coefficient. A 1% stock solution of polysorbate 20 was added to each formulation to a final polysorbate 20 concentration of 0.004% (w/v). For the IgG2, protein concentrations greater than 30 mg/mL were achieved by concentration in an Amicon Centricon Centrifugal Filter Device (Millipore, Billerica, Massachusetts) with a molecular weight cutoff of 10 K. For frozen stability studies and subsequent analysis by size-exclusion HPLC (SE-HPLC) and capillary-electrophoresis SDS (CE-SDS), volumes of the formulated protein ranging from 100  $\mu$ L to 1.25 mL (depending on the study) were stored in 3 cc glass vials. Subambient DSC was performed on 40  $\mu$ L aliquots in 50- $\mu$ L aluminum DSC pans (PerkinElmer, Waltham, Massachusetts). Time course studies were performed in both glass vials (for SE-HPLC analysis) and DSC pans (for subambient DSC measurements). Samples were stored at  $-30^\circ\text{C}$ . We originally intended to use the same primary container for both the DSC and SE-HPLC analyses, but saw high levels of clipping over time in the DSC pans (particularly in the 1 mg/mL samples at both  $-30^\circ\text{C}$  and the  $-20^\circ\text{C}$  controls), presumably because of the metal composition of the pans. It is for this reason that stability samples were stored separately in glass vials.

Stability samples formulated in sorbitol were also stored at  $-20^\circ\text{C}$  as a negative control for sorbitol crystallization, as

**Table 1.** All Formulations are 10 mM Acetate and 0.004% (w/v) Polysorbate 20

Excipient	pH	Protein Concentration (mg/mL)	Isotype
274 mM sorbitol	5.2	0.1, 1, 10, 30, 70	IgG2
274 mM sorbitol	5.2	40, 50, 60, 80, 100, 120	IgG2
274 mM sorbitol	5.2	0.1, 1, 10, 30, 70	IgG1
None	4.5	1	IgG1
300 mM sorbitol	4.5	1	IgG1
None	5.0	1	IgG1
300 mM sorbitol	5.0	1	IgG1
300 mM mannitol	5.0	1	IgG1
None	5.5	1	IgG1
300 mM sorbitol	5.5	1	IgG1

our previous work showed that sorbitol crystallizes only upon storage at  $-30^\circ\text{C}$ .<sup>12</sup> Some samples formulated in sucrose (in place of sorbitol) were included at limited time points, stored at both  $-20^\circ\text{C}$  and  $-30^\circ\text{C}$ , to assess aggregation levels in the presence of a stabilizing excipient that remains in the amorphous phase.

The sorbitol crystallization and protein aggregation of an IgG1 and IgG2 were monitored over a concentration range of 0.1–70 mg/mL. Six additional protein concentrations were analyzed for the IgG2 samples with the 70 mg/mL formulation chosen as a midpoint. In total, nine formulations were studied, including both IgG1 and IgG2 formulations ranging in protein concentration from 0.1 to 120 mg/mL and pH from 4.5 to 5.5. Proteins were formulated with 10 mM acetate at the protein concentration and pH presented in Table 1.

### Calorimetry

The subambient DSC method used to detect crystalline sorbitol melts has been described previously.<sup>12</sup> In brief, 40  $\mu$ L samples were semihermetically sealed in DSC pans and stored at  $-30^\circ\text{C}$  until analysis, when they were transferred on dry ice to a DSC cell (Pyris 1 DSC instrument, PerkinElmer, Massachusetts) that was precooled to  $-70^\circ\text{C}$ . In contrast to traditional subambient DSC methods where liquid samples are loaded and frozen by rapidly cooling to  $-70^\circ\text{C}$ , this method preserves the frozen state of the samples, which is necessary to capture the crystallization of sorbitol. The melting endotherms indicating sorbitol crystallization were integrated for total area. Sorbitol formulations stored at  $-20^\circ\text{C}$  and sucrose formulations at both  $-20^\circ\text{C}$  and  $-30^\circ\text{C}$  were included and analyzed as negative controls for sorbitol crystallization. A standard method was used to determine glass transition temperatures: a sample was aliquoted into a DSC pan, which was then placed in the DSC cell, where both the sample and DSC cell were at room temperature. Samples were cooled to  $-70^\circ\text{C}$  at a rate of  $60^\circ\text{C}/\text{min}$ , held at  $-70^\circ\text{C}$  for 1 min before heating to  $+15^\circ\text{C}$  at a rate of  $5^\circ\text{C}/\text{min}$ . Baseline slopes of the heating scans were optimized, and glass transition temperatures were calculated using the Pyris thermal analysis software for Windows, version 3.81 (PerkinElmer). The reported  $T_g'$  is the temperature at half of the change in heat capacity ( $C_p = \text{J/g } ^\circ\text{C}$ ) over the temperature range of the baseline shift.

### Chromatographic Separations

Size-exclusion HPLC was used as the primary stability indicating assay because physical instability (e.g. aggregation) is often

the dominant degradation in the frozen state.<sup>12,21–23</sup> SE-HPLC separations were performed at room temperature on an Agilent 1100 system. Chromatograms were analyzed and integrated (at either 215 or 235 nm) using Chromeleon Chromatography Data System software (Dionex Corporation, Sunnyvale, California). Chromatographic methods were optimized for each molecule analyzed. The IgG1 SE-HPLC mobile phase contained 80 mM sodium phosphate, 300 mM sodium perchlorate, and 10% isopropyl alcohol at a pH 7.2. This method used a 5- $\mu$ m particle size Tosoh TSKgel G3000SWxl 7.8 mm  $\times$  30 cm column with a 250 Å pore size (Tosoh Bioscience LLC, King of Prussia, Pennsylvania). The flow rate was 0.5 mL/min, for a total run time of 40 min, with an injection load of 21  $\mu$ g.

The IgG2 SE-HPLC method used a 5- $\mu$ m particle size Shodex KW-803 8 mm  $\times$  30 cm column with a 300 Å pore size (Showa Denko, New York, New York). The mobile phase contained 100 mM sodium phosphate and 330 mM sodium chloride at pH 6.6. The flow rate was 0.5 mL/min for a total run time of 40 min and a 30  $\mu$ g injection load.

The dimer and high-molecular-weight species (HMWS) are cointegrated as one species and reported as percent aggregate, as illustrated in Figure 1b. A frozen reference standard (stored at  $-80^{\circ}\text{C}$ ) was run at every time point to assess the performance of the SE-HPLC assay. Specifically, assay error was approximated by calculating  $\pm 2$  times the SD of the integrated aggregate peak percentage of the frozen standard obtained over 46 injections of a 21  $\mu$ g load (IgG1) or 41 injections of a 30  $\mu$ g load (IgG2) (data not shown).

Capillary electrophoresis SDS was performed on a Beckman Coulter, ProteomeLab™ PA 800 capillary electrophoresis system with photodiode array detection (Beckman Coulter, Brea, California). Electropherograms were acquired using 32 Karat™ software (Beckman Coulter); data were imported and integrated (at 220 nm) using Chromeleon Chromatography Data System software (Dionex Corporation). A single method was used for both the IgG1 and IgG2 mAbs. Samples were diluted to 0.5 mg/mL with SDS sample buffer from the Beckman Coulter SDS-MW Analysis kit (Beckman Coulter), CE grade water, and alkylated with 250 mM iodoacetamide (IAM) (Sigma, St. Louis, Missouri) for nonreduced samples. After the alkylating agent IAM was added, samples were heated in a water bath at  $70^{\circ}\text{C}$  for 4 min and cooled to room temperature before 100  $\mu$ L of each treated sample was transferred to PCR microvials. Separation was performed using 30.2 cm bare fused silica uncoated capillaries with an effective length of 20.2 cm and an inner diameter of 50  $\mu$ m. The capillary was preconditioned with 0.1 N NaOH for 3 min and 0.1 N HCl for 1 min followed by a SDS-MW gel buffer rinse for 10 min to fill the capillary; all reagents used were from Beckman Coulter. Samples were injected by reverse polarity (at 5.0 kV for 20 s), with separation at 15.0 kV for 35 min at 20 psi. Separations were performed at room temperature.

### Fragility Index Measurements

The fragility indices of IgG2 samples formulated with 10 mM acetate, pH 5.2, 274 mM sorbitol, and 0.004% (w/v) polysorbate 20 were measured at increasing protein concentrations (ranging from 0.1 to 120 mg/mL) using a TA instruments Q1000 differential scanning calorimeter (TA instruments, Newcastle, Delaware). The instrument baseline was calibrated using sapphire samples and the baseline was ensured to be devoid of

instrumental curvature or slope. The instrument temperature was calibrated using a three-point method with indium, tin, and lead as the standard samples. Heat capacity calibration was also performed in the heating mode using a sapphire standard. The liquid samples were sealed in hermetic pans and the sample sizes were between 15 and 25  $\mu$ L. The samples were initially heated to a temperature above the glass transition (typically  $T_g + 30^{\circ}\text{C}$ ) to ensure that they were in the ergodic domain. The sample was then cooled at the following rates: 15, 10, 5, 1, 0.5, and  $0.25^{\circ}\text{C}/\text{min}$  to a temperature roughly  $30^{\circ}\text{C}$  below the  $T_g'$ . The sample was held isothermally at this temperature for 3 min to ensure that the sample had transitioned to the glassy state. A standard heating rate of  $10^{\circ}\text{C}/\text{min}$  was employed to heat the glassy sample to about  $30^{\circ}\text{C}$  above its  $T_g'$ . The scan where the standard heating rate ( $10^{\circ}\text{C}/\text{min}$ ) matches the cooling rate is called the standard scan. The fictive temperature ( $T_f$ ) was computed for each cooling rate using the following expression<sup>24</sup>:

$$T_f = T_{fs} + \frac{\Delta H(Q)}{\Delta C_p} \quad (1)$$

where  $T_f$  is the derived fictive temperature at the heating rate  $Q$ ,  $T_{fs}$  is the fictive temperature for the standard scan,  $\Delta C_p$  is the specific heat capacity difference between the supercooled liquid and the glassy state for the standard scan, and  $\Delta H(Q)$  is the difference in heat between the nonstandard and standard scans for each cooling rate.  $\Delta H(Q)$  is computed by subtracting the standard scan from the DSC scan at each cooling rate. Fragility values were then computed from the fictive temperatures as described by Wang et al.<sup>24</sup> by plotting Eq. (2), where the term  $Q$  represents the cooling rate,  $Q_s$  is the standard rate ( $10^{\circ}\text{C}/\text{min}$ ), and  $m$  is fragility:

$$\log \frac{Q}{Q_s} = m - m \frac{T_{fs}}{T_f} \quad (2)$$

### Low-Temperature X-ray Diffraction

Higher concentrations of sorbitol (1.1 M) were used for X-ray diffraction (XRD) experiments to provide an improved signal-to-noise ratio for the diffraction patterns compared with the lower, isotonic concentrations of sorbitol used in our formulation stability studies (274 or 300 mM). D-Sorbitol was obtained from EMD Chemicals (Philadelphia, Pennsylvania). Approximately 400  $\mu$ L of an aqueous sorbitol solution (1.1 M, filtered through a 0.22  $\mu$ m membrane filter) was placed on a chromium-plated variable temperature XRD holder (PANalytical, Westborough, Massachusetts) and frozen at  $-30^{\circ}\text{C}$  for 3 months. At the time of analysis, the sample holder was transported on dry ice to the precooled instrument stage.

An X-ray diffractometer (X'pert MPD, PANalytical) with a variable temperature stage (TTK 450, Anton Paar, Graz, Austria) and working temperature range of  $-190^{\circ}\text{C}$  to  $450^{\circ}\text{C}$  was used. XRD patterns were obtained by exposing the sample to Cu K $\alpha$  radiation (45 kV  $\times$  40 mA). The angular range was  $3^{\circ}$ – $40^{\circ}2\theta$  at a step size of  $0.01^{\circ}2\theta$ . The sample was isothermally held for 15 min at the selected temperatures ( $-30^{\circ}\text{C}$ ,  $-20^{\circ}\text{C}$ ,  $-10^{\circ}\text{C}$ , and  $-4^{\circ}\text{C}$ ) before each scan was taken.

## RESULTS

### Sorbitol Crystallization and Protein Aggregation

Sorbitol crystallization was monitored by subambient DSC,<sup>12</sup> and Figure 1a compares the DSC thermograms of sorbitol-containing IgG1 formulations stored in DSC pans for 2 years at  $-30^{\circ}\text{C}$ . A melting endotherm indicative of sorbitol crystallization<sup>12</sup> is evident at approximately  $-8^{\circ}\text{C}$  in all 2-year samples (0.1–70 mg/mL) tested. A thermogram of the 70 mg/mL sample at time zero (bottom trace of Fig. 1a) is included for comparison because no sorbitol melt peak is evident in this sample. Note that sorbitol formulations stored at  $-20^{\circ}\text{C}$  and sucrose formulations at both  $-20^{\circ}\text{C}$  and  $-30^{\circ}\text{C}$  were included and ana-

lyzed as negative controls for sorbitol crystallization. No melting endotherms were seen in these controls (data not shown).

The rate of sorbitol crystallization and consequent protein aggregation was evaluated as a function of protein concentration during long-term frozen storage at  $-30^{\circ}\text{C}$ . Protein aggregation of the sorbitol-containing formulations was monitored by SE-HPLC. Figure 1b shows a typical SE-HPLC trace and illustrates the integration; dimer and HMWS were added together and reported as percent aggregate. Aggregation of the 0.1–70 mg/mL IgG1 sorbitol-containing formulation samples over time is shown in Figure 2a; aggregation is inversely proportional to protein concentration. The lowest protein concentration tested (0.1 mg/mL) shows the highest percent aggregate

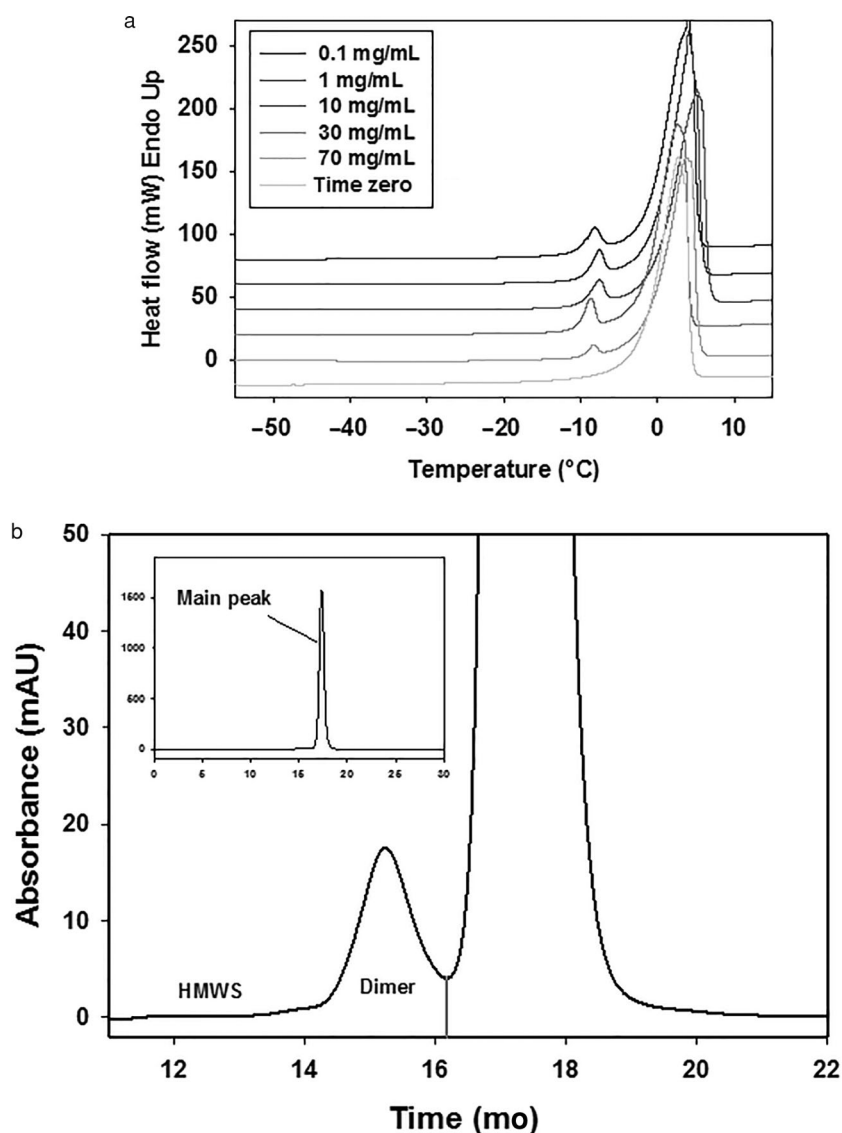


**Figure 1.** (a) Subambient DSC thermograms obtained from sorbitol-containing IgG1 formulations [10 mM acetate, pH 5.2, 274 mM sorbitol, 0.004% (w/v) polysorbate 20] stored in DSC pans at  $-30^{\circ}\text{C}$  for 2 years. Samples of increasing protein concentration displayed from top to bottom (0.1, 1, 10, 30, and 70 mg/mL). Endothermic melts are shown as positive peaks. The sorbitol endotherm melt is seen at ca.  $-8^{\circ}\text{C}$  before the ice melt peak. For comparison, a time zero trace (for the 70 mg/mL samples) is shown (bottom trace). The samples were offset for visual clarity. (b) SE-HPLC overlay of a 70 mg/mL IgG2 formulation sample formulated with 274 mM sorbitol, 10 mM acetate buffer at pH 5.2 with 0.004% (w/v) polysorbate 20, and stored at  $-30^{\circ}\text{C}$  for 24 months. The 215 nm trace is shown from 11 to 22 min; the inset shows the entire 30-min run duration and highlights the main peak. The gray line shows where the main peak integration begins (16.2 min). Dimer and high-molecular-weight species that elute before the main peak are cointegrated (from 11 to 16.2 min) and reported as one species, termed percent aggregate.



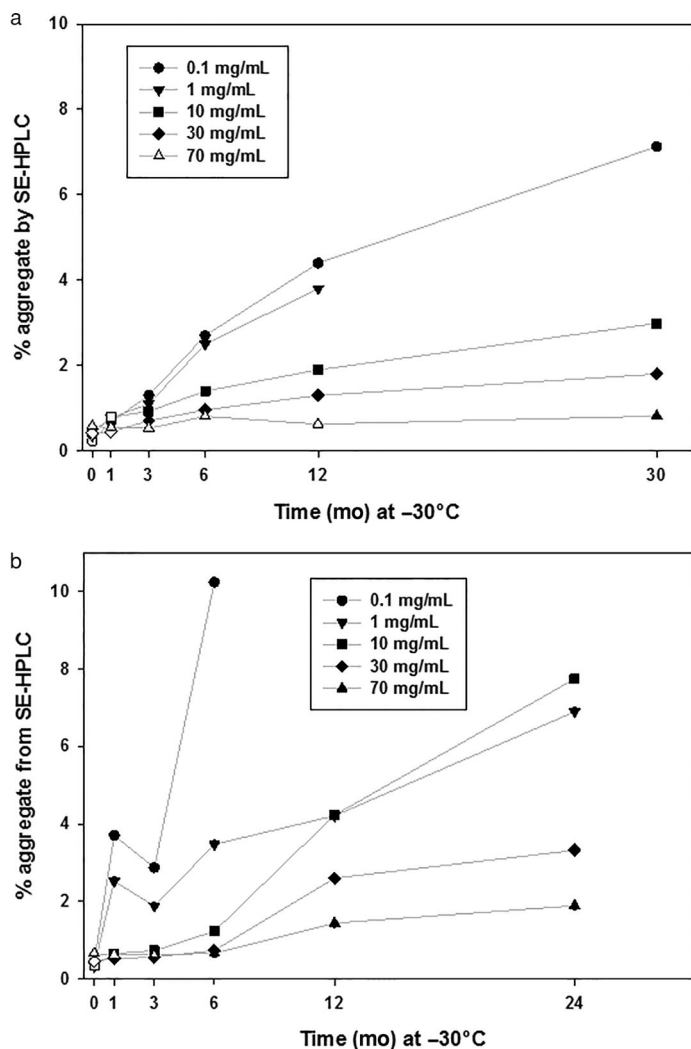


**Figure 2.** (a and b) The percent aggregate of an IgG1 (a) and IgG2 (b) shown as a function of protein concentration and time (months) at  $-30^{\circ}\text{C}$ . Samples are formulated with 10 mM acetate (pH 5.2), 274 mM sorbitol, and 0.004% (w/v) polysorbate 20. Formulation samples where sorbitol had crystallized (detected as a melting endotherm by subambient DSC) are denoted as filled symbols, whereas time points where sorbitol had not crystallized are shown as open symbols. The 1 mg/mL IgG1 sample (a) was not measured by SE-HPLC at 30 months. Note that although the 30-month SE-HPLC data point is shown, the sorbitol crystallization of these samples was assessed at 24 months. The 0.1 mg/mL IgG2 sample (b) was not tested at the 12- or 24-month time points because of sample limitations. The lines connecting the data points are meant to guide the eye; the data have not been fit to a model. For the IgG2 (b)  $t = 0$  through 6-month data reported is the average of duplicate or triplicate injections on SE-HPLC, and 12 and 24 months are single measurements. All IgG1 data (a) are single measurements.

(7.1%) after 30 months, whereas the highest IgG1 protein concentration tested (70 mg/mL) shows the lowest percent aggregate (0.8%) over the same duration of long-term frozen storage. Aggregate was also calculated in micrograms, and the rank order of highest to lowest aggregate was the same as in Figure 2a (data not shown).

Protein aggregation was also assessed in IgG2 formulations (Figs. 2b and 3). The percent aggregate for 0.1–70 mg/mL sorbitol-containing formulations over 24 months of frozen stor-

age is shown in Figure 2b. Again, aggregation is inversely proportional to protein concentration. The 0.1 mg/mL sample showed the largest increase in percent aggregate (9.8% increase over 6 months of frozen storage), whereas the 70 mg/mL IgG2 formulation sample showed a 1.2% increase in percent aggregate over a fourfold longer duration at  $-30^{\circ}\text{C}$  (i.e., 24 months of frozen storage). Note that although the 10 and 1 mg/mL samples showed a similar percent aggregate after 1 year at  $-30^{\circ}\text{C}$ , by 24 months of frozen storage, the 10 mg/mL sample shows slightly higher percent aggregate compared with the 1 mg/mL sorbitol-containing formulation. As determined by subambient DSC, sorbitol crystallized in the 0.1, 1, 10, and 30 mg/mL IgG2 formulations after 1-month storage at  $-30^{\circ}\text{C}$ , whereas the 70 mg/mL IgG2 sorbitol-containing formulation showed evidence of partial sorbitol crystallization after 6 months of frozen storage. Minimal increase in the percent aggregate is seen in both 70 mg/mL formulations tested, despite the fact that sorbitol crystallized at 6 months in the IgG2 formulation (Fig. 2b) and not until 24 months in the IgG1 formulation (Fig. 2a). Aggregate was also calculated in micrograms, and the rank order of highest to lowest aggregate was the same as in Figure 2b (data not shown).

The aggregation of 40, 50, 60, 80, 100, and 120 mg/mL sorbitol-containing IgG2 formulation samples over 24 months at  $-30^{\circ}\text{C}$  is shown in Figure 3. An increase in aggregation is seen in the 40, 50, and 60 mg/mL formulations where sorbitol crystallization was detected, whereas the 80, 100, and 120 mg/mL samples do not undergo significant (i.e.,  $>10\%$ ) crystallization of sorbitol based on integrated sorbitol melt peaks, if present, and showed a little increase in aggregate (by SE-HPLC) after 2 years at  $-30^{\circ}\text{C}$ . As previously described, calculating the aggregate in terms of micrograms showed the same rank order as shown in Figure 3 (data not shown).

### Effect of pH

To determine the role of pH in the aggregation of sorbitol-containing protein formulations during long-term storage at  $-30^{\circ}\text{C}$ , the physical stability of an IgG1 at 1 mg/mL was monitored in the buffering range of acetate from pH 4.5 to 5.5. This study was conducted at a low protein concentration because sorbitol is expected to be fully crystallized in these samples for almost the entire duration of frozen storage (crystallization was detected in the 1 mg/mL samples after 3 days at  $-30^{\circ}\text{C}$  (data not shown)). As shown in Figure 4, after  $-30^{\circ}\text{C}$  storage for 30 months, aggregation was highest at pH 4.5 at 15.1%, whereas the pH 5.0 and 5.5 sorbitol-containing formulations showed less aggregate at 4.5% and 4.3%, respectively.

To compare the long-term frozen protein stability of formulations after the crystallization of an excipient with protein formulations lacking excipient, the stability of an IgG1 formulated without excipient was also monitored as a function of pH (Fig. 5). In addition, a mannitol formulation sample was included as a control to monitor the stability of the IgG1 in the presence of an excipient known to crystallize readily upon freezing (mannitol samples are designated by filled symbols in Fig. 5). As shown in Figure 5, the pH 4.5 formulation without excipient showed the greatest percent aggregate (16.2%) after 30 months at  $-30^{\circ}\text{C}$ , whereas the pH 5.0 and 5.5 samples without excipient showed the least (1.3% and 1.4%, respectively). Aggregation levels at pH 5.0 and 5.5 were similar, and formulations without excipient showed less aggregate than those

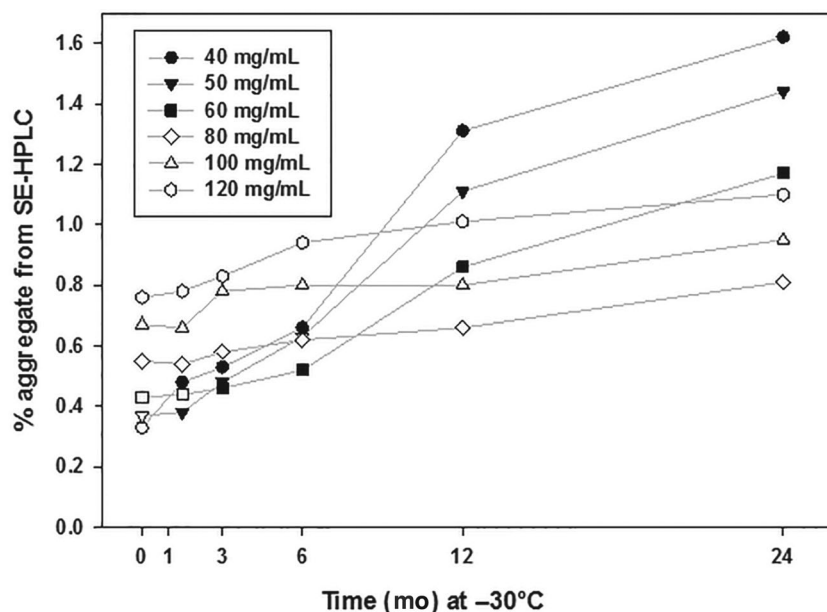


**Figure 3.** The percent aggregate of an IgG2 (from SE-HPLC) over 24 months at  $-30^{\circ}\text{C}$  is shown as a function of protein concentration. All samples are formulated with 10 mM acetate (pH 5.2), 274 mM sorbitol, and 0.004% (w/v) polysorbate 20. Formulation samples where sorbitol had crystallized (detected as a melting endotherm by subambient DSC) are denoted with filled symbols. After 1 year of frozen storage at  $-30^{\circ}\text{C}$ , the 80 and 100 mg/mL samples showed evidence of a small sorbitol melt peak on subambient DSC, but because the peak areas showed less than 10% sorbitol crystallization, neither sample was designated as having crystallized. The average of duplicate injections is shown from  $t = 0$  through 12 months, and single measurements are shown at 24 months.

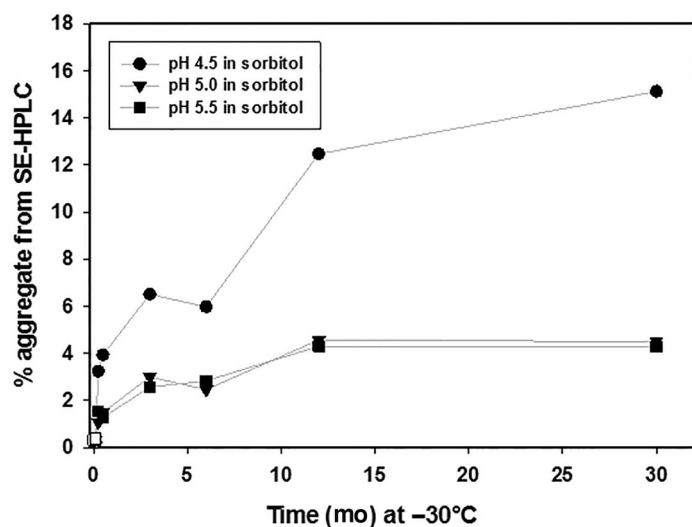


**Figure 4.** The percent aggregate (from SE-HPLC) of 1 mg/mL IgG1 formulation samples over 30 months of frozen storage at  $-30^{\circ}\text{C}$  is shown as a function of pH. All samples contain 300 mM sorbitol with 10 mM acetate (pH 4.5, 5, or 5.5) and 0.004% (w/v) polysorbate 20. Sorbitol crystallization occurred in all sorbitol-containing formulations shown after 1 week at  $-30^{\circ}\text{C}$ , as denoted by filled symbols. The average of two injections at  $t = 0$  is reported; all other time points are single measurements.

containing sorbitol. Moreover, the pH 5.0 and 5.5 sorbitol-containing formulations (Fig. 4) showed lower aggregate levels (4.5% and 4.3%, respectively) than the mannitol formulation at pH 5.0 (6.3%).

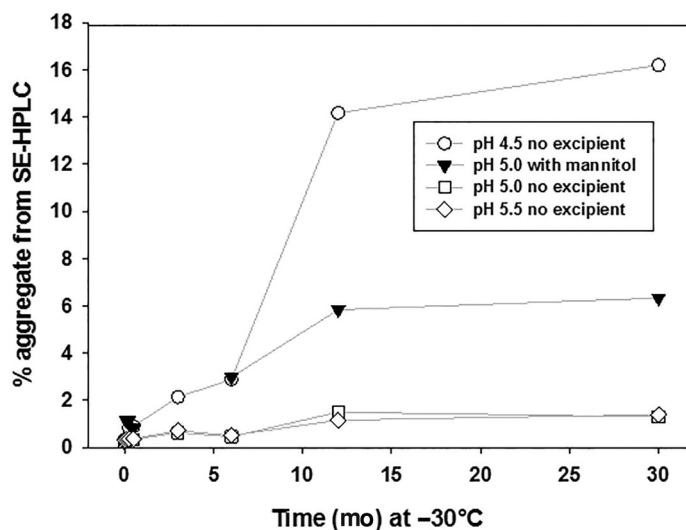


**Figure 5.** The percent aggregate of an IgG1 (from SE-HPLC) over 30 months of frozen storage at  $-30^{\circ}\text{C}$  is shown as a function of pH in the absence of excipient. All samples are formulated at a concentration of 1 mg/mL with 10 mM acetate at pH 4.5, 5, or 5.5, and 0.004% (w/v) polysorbate 20. One formulation contained 300 mM mannitol and is shown by filled symbols denoting that mannitol crystallized upon freezing. The average of two injections at  $t = 0$  is reported.

### Characterization of the Aggregate Species

The aggregate resulting from sorbitol crystallization of the 1 mg/mL IgG1 samples was assessed by nonreduced CE-SDS

(NR CE-SDS) after 1 year at  $-30^{\circ}\text{C}$  and compared with formulations at the same pH in the absence of excipient (data not shown). Because a little increase in aggregate was seen between the 12- and 30-month time points (by SE-HPLC, Figs. 4 and 5), these samples were not reanalyzed by NR CE-SDS after 30 months of frozen storage. The covalent aggregate by NR CE-SDS was less than 1% for all samples analyzed (data not shown), suggesting the aggregate is predominantly noncovalent.

#### Characterization of the Frozen State: Measurement of $T_g'$ of Amorphous Sorbitol and Fragility Indices

In the frozen state, an amorphous excipient can undergo a viscoelastic transition from a rubbery to a more viscous glassy state, which is characterized by a  $T_g'$  measured by subambient DSC<sup>5,11,25,26</sup> (note that the glass transition measurements were made at  $t = 0$  from the liquid state). Therefore, in these samples that were rapidly cooled, sorbitol remained amorphous. The  $T_g'$  reported for sorbitol is  $-44^{\circ}\text{C}$ .<sup>11</sup> Figure 6 shows the  $T_g'$  as a function of protein concentration for the IgG1 and IgG2 sorbitol-containing formulations shown in Figures 2a, 2b, and 3. At the lower protein concentrations, the  $T_g'$  is influenced primarily by the excipient sorbitol. The  $T_g'$  increases linearly with increasing protein concentration. The formulations  $\geq 100$  mg/mL show glass transition temperatures above the  $-30^{\circ}\text{C}$  storage condition (shown as a horizontal line in Fig. 6).

Figure 7a shows the fragility index as a function of protein concentration for the 0.1–120 mg/mL IgG2 sorbitol-containing formulations shown in Figures 2b and 3. The fragility index value can be determined from either the slope or the intercept of the plot of Eq. (2), shown in the *Materials and Methods* section. This is illustrated by Figure 7b, which shows a plot of scaled cooling rate ( $\log(Q/Q_s)$ ) versus scaled fictive temperature ( $T_{fs}/T_f$ ) for the 120 mg/mL sample. Fragility index values decreased as a function of protein concentration (Fig. 7a), which

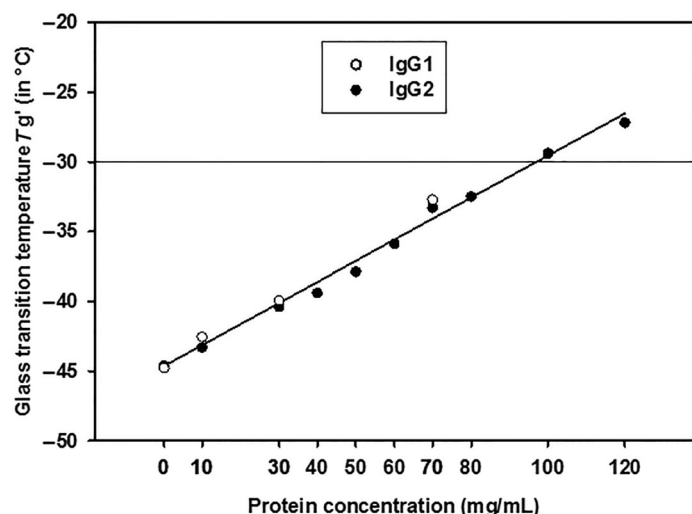


**Figure 6.** The glass transition temperature ( $T_g'$ ) of an IgG1 (indicated by open circles) and IgG2 (indicated by filled circles) formulated with 10 mM acetate at pH 5.2, 274 mM (5% w/v) sorbitol, and 0.004% (w/v) polysorbate 20 is shown as a function of increasing protein concentration (0, 0.1, 1, 10, 30, 40, 50, 60, 70, 80, 100, and 120 mg/mL). The line at  $-30^{\circ}\text{C}$  highlights the  $-30^{\circ}\text{C}$  storage temperature. The data were fit by linear regression, and the resulting  $R^2$  value was 0.989.

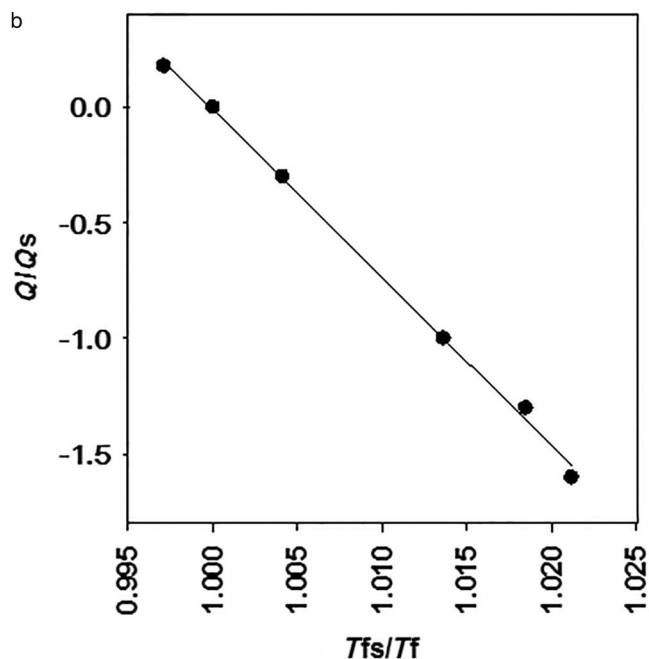
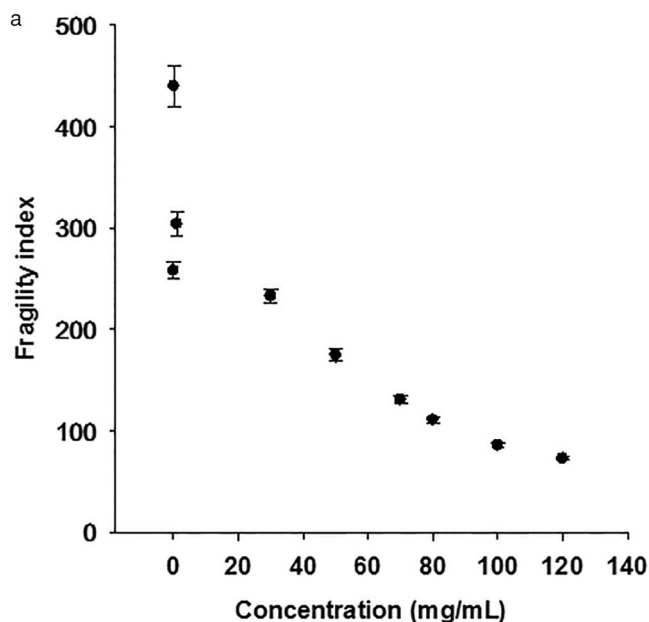


**Figure 7.** (a) Fragility index as a function of IgG2 protein concentration of sorbitol-containing formulations [10 mM acetate, pH 5.2, 274 mM sorbitol, and 0.004% (w/v) polysorbate 20]. The protein concentrations monitored are 0, 0.1, 1, 30, 50, 70, 80, 100, and 120 mg/mL. (b) The plot of scaled cooling rate versus scaled fictive temperature for the IgG2 at a protein concentration of 120 mg/mL is shown. Both the slope and the intercept of the graph indicate the fragility index calculated for the 120 mg/mL sample using Eq. (2).

suggests reduced dynamic heterogeneity in the sample as the protein concentration increased.

#### Characterization of Crystalline Sorbitol

X-ray diffraction provides a direct measurement of crystalline sorbitol. This technique is complementary to subambient DSC, where the crystallinity of sorbitol is inferred through the

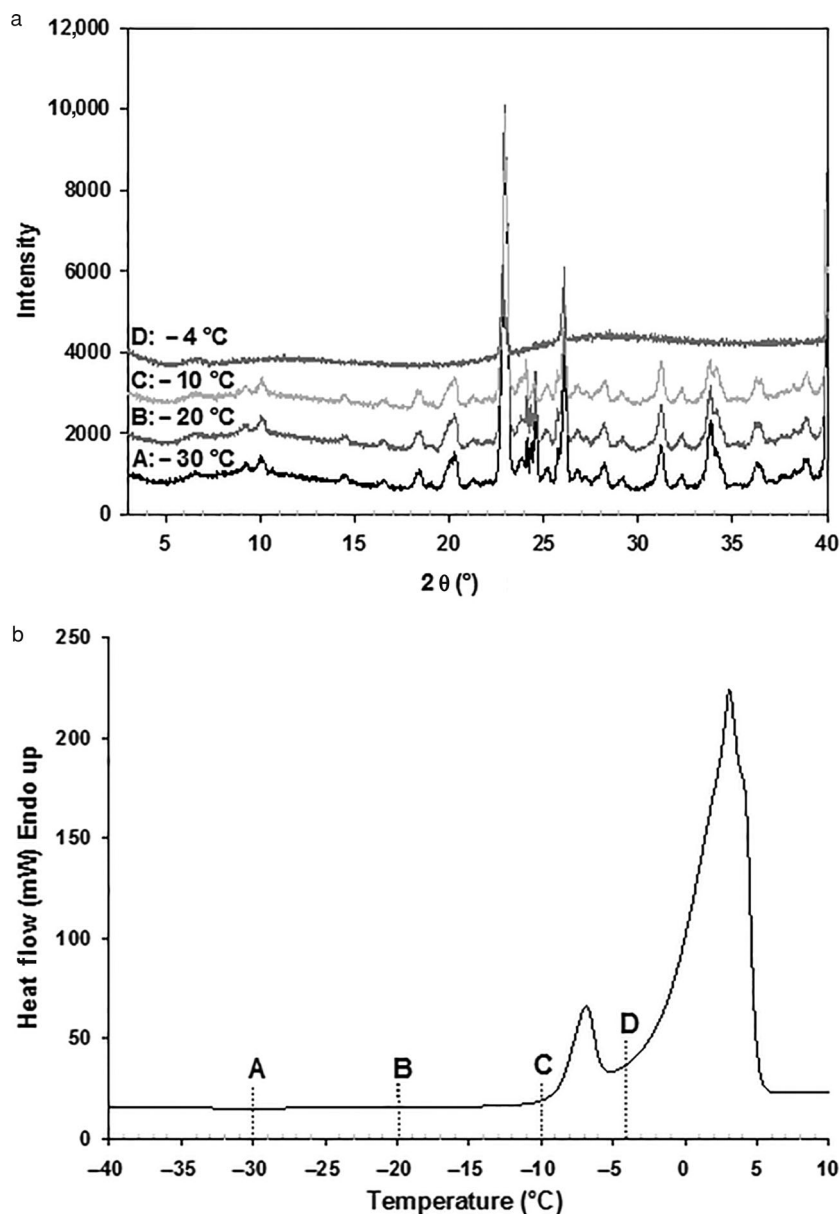


**Figure 8.** (a) Variable-temperature X-ray diffraction (XRD) patterns collected for a 1.1 M sorbitol solution that was stored frozen for 3 months at  $-30^{\circ}\text{C}$ . XRD traces were collected at A,  $-30^{\circ}\text{C}$ ; B,  $-20^{\circ}\text{C}$ ; C,  $-10^{\circ}\text{C}$ ; and D,  $-4^{\circ}\text{C}$ . (b) Subambient DSC thermogram for a 274 mM sorbitol solution stored in DSC pans at  $-30^{\circ}\text{C}$  for 1 week. The dashed lines represent the temperatures at which XRD patterns were collected for the 1.1 M sorbitol solution as shown in panel (a).

observation of a crystalline melt. Figure 8a shows the XRD diffractograms of a 1.1 M sorbitol sample as a function of temperature from  $-30^{\circ}\text{C}$  to  $-4^{\circ}\text{C}$ . The XRD patterns show that sorbitol is crystalline at the frozen temperatures monitored up to  $-10^{\circ}\text{C}$ . However, by  $-4^{\circ}\text{C}$ , the crystalline structure no longer persists and the remaining peaks are from ice. The identification of the sorbitol polymorphs has not been trivial and work is ongoing. Figure 8b shows the subambient DSC thermogram of a 274 mM sorbitol solution stored at  $-30^{\circ}\text{C}$  for a week. The temperatures at which XRD patterns were collected ( $-30^{\circ}\text{C}$ ,  $-20^{\circ}\text{C}$ ,  $-10^{\circ}\text{C}$ , and  $-4^{\circ}\text{C}$ ) are labeled as A, B, C, and D, respectively, as shown in Figure 8b. By XRD, sorbitol remains crystalline at  $-10^{\circ}\text{C}$  but is no longer crystalline at  $-4^{\circ}\text{C}$ , correlating with subambient DSC data that shows the sorbitol polymorph melt at ca.  $-8^{\circ}\text{C}$ .

## DISCUSSION

Sorbitol crystallization and consequent protein aggregation were monitored for IgG1 and IgG2 mAbs as a function of protein concentration during long-term frozen storage at  $-30^{\circ}\text{C}$ . An inverse dependence of aggregation on protein concentration is evident. In formulation samples where sorbitol crystallized, a time-dependent lag in aggregation is seen. This “lag phase,” where aggregate levels increase after 3–6 months of frozen storage, is apparent in both mAbs tested (Figs. 2a, 2b, and 3). Therefore, for low protein concentration formulations, short-term frozen data may not necessarily be predictive of stability at later time points. Higher protein concentration formulation samples (80, 100, and 120 mg/mL) start out with a higher percent aggregate, presumably because of molecular crowding.<sup>27,28</sup>



However, these formulations show little increase in aggregate ( $\leq 0.3\%$ ) over 24 months, likely because these samples underwent minimal sorbitol crystallization (Fig. 3). Because excipient crystallization precedes increased protein aggregation, a method that could predict the propensity for sorbitol-containing formulations to crystallize upon long-term frozen storage could be useful. Understanding the potential of an amorphous excipient to crystallize is increasingly relevant for mAbs because it can result in instability during frozen storage, as shown here and by others. Sundaramurthi et al.<sup>7</sup> characterized trehalose crystallization in a frozen solution, which resulted in the instability of a mAb stored frozen, as reported by Singh et al.<sup>29</sup>

In addition to the dependence of sorbitol crystallization-induced aggregation on protein concentration, the kinetics of sorbitol crystallization also varied as a function of protein concentration. Specifically, crystallization rates were fastest (on the order of hours) for sorbitol samples without protein, particularly at sorbitol concentrations greater than 300 mM (data not shown), and ranged from weeks to months for the protein-containing sorbitol formulations depending on the protein concentration. Complete sorbitol crystallization is evident by the area of the sorbitol melting endotherm on DSC and is typically greater than 400 mJ for a 274 mM sorbitol formulation.<sup>12</sup> Note that the threshold concentration above which the crystalline sorbitol melt can be detected by subambient DSC is ca. 50 mM (data not shown). As shown in Figure 1a, the area under the sorbitol melt peak at ca.  $-8^{\circ}\text{C}$  is similar for the 0.1, 1, 10, and 30 mg/mL 2-year samples (average of  $422 \pm 10$  mJ), whereas the sorbitol melt peak for the 70 mg/mL 2-year time point is threefold lower at 127 mJ, suggesting sorbitol in the 70 mg/mL IgG1 formulation sample has not completely crystallized. Differences in the rates of sorbitol crystallization were noted both between the different mAb isotypes and sometimes while monitoring the same mAb in different studies. For example, the 70 mg/mL IgG2 sorbitol-containing formulation showed evidence of sorbitol crystallization after 6 months at  $-30^{\circ}\text{C}$  (Fig. 2b), whereas the same protein concentration IgG1 formulation did not show evidence of sorbitol crystallization until 2 years at  $-30^{\circ}\text{C}$  (Fig. 2a). The difference in crystallization rates may be because of a combination of factors: the stochastic nature of nucleation, perhaps partially arising from differences in sample preparation because particles can nucleate ice formation<sup>30</sup> and/or differences in cooling rates because of uncontrolled freezing in our laboratory freezers. Interestingly, the polymorph distribution of mannitol has been reported to change both as a function of freezing rate and mannitol concentration.<sup>31</sup> We chose not to use controlled-rate freezers in these experiments because controlled rate freezers are typically not used in our cold-chain storage and we wanted our sample handling to be more representative of real-life conditions.

A trend of delayed sorbitol crystallization in higher protein concentration formulations is apparent throughout our studies (Figs. 2a, 2b, and 3). We propose this is in part because of decreased molecular mobility at higher protein concentrations. The glass transition temperatures of the 0.1–120 mg/mL formulations increase linearly with protein concentration (Fig. 6), as a function of the weight ratio of protein to solute. Carpenter et al.<sup>32</sup> reported that protein present at greater than 20% (w/w) can have a large effect on the  $T_g'$  of the formulation, and estimated the  $T_g'$  of pure protein solutions to be ca.  $-10^{\circ}\text{C}$ . Liao et al.<sup>33</sup> also reported a marked increase in  $T_g'$  at protein concentrations greater than 20 mg/mL. As shown in Figure 6,

the  $T_g'$  of protein concentrations greater than 70 mg/mL approach  $-30^{\circ}\text{C}$ , the temperature at which sorbitol crystallization occurs. Increased  $T_g'$  values suggest that higher protein concentration formulations have decreased molecular mobility at  $-30^{\circ}\text{C}$ . Bhugra et al.<sup>34</sup> proposed that crystallization in the amorphous phase is related to molecule mobility, meaning a correlation between relaxation times and crystallization onsets (above  $T_g'$ ) could potentially be used to predict the onset temperature of crystallization.

Slower sorbitol crystallization in high protein concentration formulations may be caused by the protein interfering in the crystallization of sorbitol. Liao et al.<sup>33</sup> reported that a mAb inhibited mannitol crystallization in a protein concentration-dependent manner. The authors reported that the mAb inhibited both the nucleation and growth of mannitol crystals. In fact, the suppression of crystallization by formulation components is reported throughout the literature; polymers are often used to inhibit small molecule crystallization during formulation. Even at low concentrations, salts such as NaCl are known to interfere with mannitol crystallization.<sup>31,33,35</sup>

Higher protein aggregation levels were seen at the low formulation pH values tested (shown in Figs. 4 and 5). Kueltzo et al.<sup>36</sup> also reported increased aggregation (induced by freeze–thaw cycling) of an IgG2 at lower pH formulations. The authors studied a broad pH range of 3–8 and reported that aggregation of the antibody during freeze–thawing increased with decreasing pH.<sup>36</sup>

Protein aggregation at  $-30^{\circ}\text{C}$  was monitored in the presence (Fig. 4) and absence (Fig. 5) of sorbitol as a function of pH and compared with a formulation containing mannitol, an excipient that readily crystallizes upon freezing. After 30 months at  $-30^{\circ}\text{C}$ , a fourfold increase in aggregate (by SE-HPLC) was seen in the pH 5.0 mannitol-containing formulation compared with the same sample formulated in the absence of excipient. Similarly, samples formulated with sorbitol that underwent crystallization showed higher aggregate levels upon long-term frozen storage compared with samples at the same pH but formulated without an excipient. This trend holds at pH 5.0 and 5.5, although at pH 4.5 the formulation without excipient showed slightly higher aggregation levels than the sorbitol-containing formulation (16.2% and 15.1% aggregate, respectively). Under the conditions tested, the crystallization of sorbitol destabilizes the protein to a greater extent than the same formulations stored frozen without excipient. Sorbitol has a protein-stabilizing effect in the liquid state and in the frozen state, as long as the protein and excipient are in the same phase. The crystallization of sorbitol upon long-term frozen storage at  $-30^{\circ}\text{C}$  resulting in its phase separation from protein is more detrimental to protein stability than frozen storage in the absence of excipient. Sorbitol provides a stabilizing interaction that, once removed, leads to increased protein aggregation. Moreover, the hydrogen bonding potential of sorbitol depends on temperature and whether the excipient is in the glassy or amorphous phase.<sup>37</sup> At 1 mg/mL, aggregation occurred fairly rapidly upon  $-30^{\circ}\text{C}$  storage, which was not the case for higher concentration formulations that exhibited a lag between sorbitol crystallization and subsequent aggregation.

Cosolvents have been reported to influence excipient crystallization, which is an especially relevant consideration for lyophilized formulations that contain multiple excipients (e.g., the bulking agent mannitol and lyoprotectants sucrose and trehalose).<sup>38</sup> Moreover, citrate and trisodium and tripotassium

phosphates have been reported to suppress the crystallization of mannitol.<sup>39</sup> Here, we did not explore the influence of cosolutes on the crystallization of sorbitol because our formulation was not a lyophilized formulation, and sorbitol was the sole stabilizing excipient in an acetate buffer. In experiments wherein mannitol was used (Fig. 5), it was the sole excipient and used as a positive control for excipient crystallization.

Our initial DSC work suggested the presence of two sorbitol polymorphs: a metastable form with a melting temperature of  $-20^{\circ}\text{C}$  that persisted up to 4 weeks,<sup>12</sup> and the presumably more stable form with a melting temperature of ca.  $-8^{\circ}\text{C}$  that was evident after as little as 2 weeks and was the sole endotherm seen beyond 4 weeks storage at  $-30^{\circ}\text{C}$  (Figs. 1a and 8b). DSC thermograms showing a metastable polymorph converting to a more stable form has been reported for several molecules (e.g., iopanoic acid, carbamazepine, piroxicam, and pirenanide).<sup>40</sup> Seven crystalline sorbitol forms have been identified at room temperature: two hydrates and five anhydrous forms (termed A,  $\beta$ ,  $\Gamma$ ,  $\Delta$ , and E).<sup>41</sup> Three of these forms (A, E, and hydrate I) have been identified from single-crystal XRD data.<sup>41</sup> XRD results suggest that the crystalline sorbitol polymorph persists to frozen temperatures as warm as  $-10^{\circ}\text{C}$ , but is no longer crystalline at  $-4^{\circ}\text{C}$ . These diffraction patterns (Fig. 8a) correlate with thermal events seen by subambient DSC (Fig. 8b), where the melting of the sorbitol polymorph is detected at ca.  $-8^{\circ}\text{C}$ . Characterization of the sorbitol polymorph is ongoing, and is beyond the scope of this work. Characterization and quantitation of crystalline trehalose required the refinement of vibrational spectroscopic methods such as dispersive Raman spectroscopy and near-infrared diffuse resonance spectroscopy, and multivariate analysis of the resulting data.<sup>42</sup>

Tanaka et al.<sup>43–46</sup> have published on the origins of fragility differences in glasses. Their theoretical studies use a two-order-parameter model of liquids and molecular dynamics simulations and have suggested a strong correlation between short-range ordering in liquids and fragility. They postulated that strong glass formers have an inherent short-range order, whereas fragile glasses are devoid of such local order.<sup>44–46</sup> For strong glasses, this implies that there are locally favored structures that have sufficient lifetimes and local symmetries that are conserved when the equilibrium supercooled liquid passes over to the nonequilibrium glass at the  $T_g'$ . Furthermore, measuring the fragility index helps to normalize system dynamics close to  $T_g'$ , making it a useful tool to compare the same formulation at different protein concentrations and therefore different  $T_g'$ s. The fragility indices of frozen sorbitol-containing formulations over a broad range of protein concentrations (0.1–120 mg/mL) were measured and are shown in Figure 7a.

The fragility indices measured for 0.1 and 1 mg/mL solutions are higher than the fragility index for sorbitol in the buffer alone (Fig. 7a). Thus, the system dynamics (with respect to mobility) near  $T_g'$  are accelerated at protein concentrations of 0.1 and 1 mg/mL compared with the same sorbitol formulation in the absence of protein. However, as the protein concentration reaches 30 mg/mL, the fragility index drops below the value for sorbitol in buffer. Fragility indices decreased as the protein concentration increased, suggesting that increasing protein concentration substantially retards system dynamics at the  $T_g'$ . Above 70 mg/mL, there is more protein by weight than sorbitol. As the protein concentration increased, both the weight ratio of protein to sorbitol and the  $T_g'$  increased (Fig. 6), and likely served to retard sorbitol crystallization. Because of sys-

tem mobility, it was increasingly difficult to crystallize sorbitol in a frozen formulation as the protein concentration increased. At high protein concentrations, the fragility values of protein–sorbitol mixtures appear to level off because little change is seen in the fragility values between 100 and 120 mg/mL (Fig. 7a).

The fragility data correlated with sorbitol crystallization data from long-term stability studies at  $-30^{\circ}\text{C}$  in that sorbitol crystallization was only observed in systems of higher fragility. For the systems in this study, the storage temperature of  $-30^{\circ}\text{C}$  is close to or above the  $T_g'$ , meaning crystallization of excipient near  $T_g'$  is being investigated. Crystallization rate of small molecule organics in the supercooled liquid state above  $T_g'$  correlates well with molecular mobility. However, crystallization rate in glasses close to and below  $T_g'$  does not correlate well with bulk mobility because other mechanisms such as surface crystallization are dominant. Because fragility is essentially connected with mobility in the liquid, it may be able to predict crystallization above  $T_g'$ ; however, predicting crystallization in the glassy state is challenging. Scopigno et al.<sup>47</sup> have shown that kinetic fragility correlates well with glass fragility. Thus, measurements from the liquid side can be extended to the glassy state. Because the correlation between fragility itself and the potential for excipient crystallization is not yet universally established, additional work would be needed to see whether this implication would hold for other systems. If such correlations hold, then the advantage of measuring fragility becomes apparent as it is a rapid technique as opposed to long-term stability assessments.

## CONCLUSIONS

Sorbitol crystallization can affect the stability of frozen mAb formulations; we monitored sorbitol crystallization and consequent protein aggregation in different formulation conditions such as protein concentration and pH. After sorbitol crystallization, the physical stability of the mAb, essentially in the absence of excipient, is driven by the inherent stability of the molecule in its formulation condition, which is primarily determined by formulation pH and protein concentration. Increased aggregation was seen at the lower pH formulations tested, suggesting that a judicious choice of formulation pH is the key to ensure adequate frozen stability of sorbitol-containing formulations. Higher protein concentration formulations showed less aggregation likely because of a decreased mobility in the frozen state (as shown by  $T_g'$  measurements), suppression of sorbitol crystallization by the protein itself,<sup>33</sup> and high protein concentration formulations may be self-stabilizing. The lag time between sorbitol crystallization and subsequent aggregation (where aggregation levels increase after 6 months) suggests that to accurately assess stability trends of sorbitol-containing formulations stored at  $-30^{\circ}\text{C}$ , the stability of these formulations must be assessed in long term. Measuring the fragility index of formulations can perhaps provide a complementary approach to gain insight into dynamic heterogeneity in systems of varying protein concentration as the glass transition is traversed from the liquid side. Our results suggest that sorbitol crystallization and subsequent aggregation is less of a concern at higher protein concentrations, where the protein is presumably self-stabilizing and the sorbitol crystallization is delayed. Even with its propensity to crystallize in the frozen

state, sorbitol is an efficient stabilizing excipient in the liquid state.

## ACKNOWLEDGMENTS

The authors are grateful to Arnold McAuley for DSC expertise and helpful discussions; Sabine Hogan for her assistance with the VP-DSC instrumentation, data collection, and integration; April McDonald Davison, Belqis Samady, Haley Bacon, and Lyanne Wong for SEC methodology and data; Vasumathi Dharmavaram for assistance with data visualization; Christie Summers for supporting work on the N-terminal fusion protein; Margaret Ricci, Michael Treuheit, and Stephen Brych for support and critical review of the manuscript.

## REFERENCES

- Randolph TW. 1997. Phase separation of excipients during lyophilization: Effects on protein stability. *J Pharm Sci* 86(11):1198–1203.
- Privalov PL. 1990. Cold denaturation of proteins. *Crit Rev Biochem Mol Biol* 25(4):281–305.
- Franks F. 1995. Protein destabilization at low temperatures. *Adv Protein Chem* 46:105–139.
- Strambini GB, Gabellieri E. 1996. Proteins in frozen solutions: Evidence of ice-induced partial unfolding. *Biophys J* 70(2):971–976.
- Chang LL, Shepherd D, Sun J, Ouellette D, Grant KL, Tang XC, Pikal MJ. 2005. Mechanism of protein stabilization by sugars during freeze-drying and storage: Native structure preservation, specific interaction, and/or immobilization in a glassy matrix? *J Pharm Sci* 94(7):1427–1444.
- Pikal M. 1994. Freeze drying of proteins. In *Stability, formulation and delivery of peptides and proteins*; Cleland J, Langer R, Eds. Washington, DC: American Chemical Society, pp 120–133.
- Sundaramurthi P, Patapoff TW, Suryanarayanan R. 2010. Crystallization of trehalose in frozen solutions and its phase behavior during drying. *Pharm Res* 27(11):2374–2383.
- Herman AC, Boone TC, Lu HS. 1996. Characterization, formulation, and stability of Neupogen (Filgrastim), a recombinant human granulocyte-colony stimulating factor. *Pharm Biotechnol* 9:303–328.
- Piedmonte DM, Treuheit MJ. 2008. Formulation of Neulasta (pegfilgrastim). *Adv Drug Deliv Rev* 60(1):50–58.
- Levine H, Slade L. 1988. Thermomechanical properties of small-carbohydrate-water glasses and 'rubbers'. *J Chem Soc Faraday Trans* 84:2619–2633.
- Costantino H. 2004. Excipients for use in lyophilized pharmaceutical peptide, protein and other bioproducts. In *Lyophilization of biopharmaceuticals*; Costantino H, Pikal M, Eds. Arlington, Virginia: AAPS, pp 139–228.
- Piedmonte DM, Summers C, McAuley A, Karamujic L, Ratnaswamy G. 2007. Sorbitol crystallization can lead to protein aggregation in frozen protein formulations. *Pharm Res* 24(1):136–146.
- Hu L, Ye F. 2014. Liquid fragility calculations from thermal analyses for metallic glasses. *J Non-Cryst Solids* 386:46–50.
- Ramos JJM, Taveira-Marques R, Diogo HP. 2004. Estimation of the fragility index of indomethacin by DSC using the heating and cooling rate dependency of the glass transition. *J Pharm Sci* 93(6):1503–1507.
- Velikov V, Borick S, Angell CA. 2002. Molecular glasses with high fictive temperatures for energy landscape evaluations. *J Phys Chem B* 106(5):1069–1080.
- Angell CA. 1995. Formation of glasses from liquids and biopolymers. *Science* 267(5206):1924–1935.
- Ikeda M, Aniya M. 2010. Correlation between fragility and cooperativity in bulk metallic glass-forming liquids. *Intermetallics* 18(10):1796–1799.
- Ndeugueu JL, Ikeda M, Aniya M. 2010. Correlation between the temperature range of cooperativity and the fragility index in ion-conducting polymers. *Solid State Ionics* 181(1–2):16–19.
- Torchinsky DH, Johnson JA, Nelson KA. 2009. A direct test of the correlation between elastic parameters and fragility of ten glass formers and their relationship to elastic models of the glass transition. *J Chem Phys* 130(6):064502/064501–064502/064511.
- Wang L-M. 2009. Enthalpy relaxation upon glass transition and kinetic fragility of molecular liquids. *J Phys Chem B* 113(15):5168–5171.
- Arakawa T, Kita Y, Carpenter JF. 1991. Protein–solvent interactions in pharmaceutical formulations. *Pharm Res* 8(3):285–291.
- Bhatnagar BS, Bogner RH, Pikal MJ. 2007. Protein stability during freezing: Separation of stresses and mechanisms of protein stabilization. *Pharm Dev Technol* 12(5):505–523.
- Carpenter JF, Kendrick BS, Chang BS, Manning MC, Randolph TW. 1999. Inhibition of stress-induced aggregation of protein therapeutics. *Methods Enzymol* 309:236–255.
- Wang L, Velikov V, Angell CA. 2002. Direct determination of kinetic fragility indices of glassforming liquids by differential scanning calorimetry: Kinetic versus thermodynamic fragilities. *J Chem Phys* 117(22):10184–10355.
- Carpenter JF, Crowe JH. 1988. The mechanism of cryoprotection of proteins by solutes. *Cryobiology* 25(3):244–255.
- Franks F. 1993. Solid aqueous solutions. *Pure Appl Chem* 65(12):2527–2537.
- Minton AP. 2005. Influence of macromolecular crowding upon the stability and state of association of proteins: Predictions and observations. *J Pharm Sci* 94(8):1668–1675.
- Zimmerman S, Minton A. 1993. Macromolecular crowding: Biochemical, biophysical, and physiological consequences. *Annu Rev Biophys Biomol Struct* 22:27–65.
- Singh SK, Kolhe P, Mehta AP, Chico SC, Lary AL, Huang M. 2011. Frozen state storage instability of a monoclonal antibody: Aggregation as a consequence of trehalose crystallization and protein unfolding. *Pharm Res* 28(4):873–885.
- Han X, Ma HB, Wilson C, Critser JK. 2008. Effects of nanoparticles on the nucleation and devitrification temperatures of polyol cryoprotectant solutions. *Microfluid Nanofluidics* 4(4):357–361.
- Kim AI, Akers MJ, Nail SL. 1998. The physical state of mannitol after freeze-drying: Effects of mannitol concentration, freezing rate, and a noncrystallizing cosolute. *J Pharm Sci* 87(8):931–935.
- Carpenter JF, Pikal MJ, Chang BS, Randolph TW. 1997. Rational design of stable lyophilized protein formulations: Some practical advice. *Pharm Res* 14(8):969–975.
- Liao X KR, Suryanarayanan R. 2005. Influence of the active pharmaceutical ingredient concentration on the physical state of mannitol-implications in freeze-drying. *Pharm Res* 22(11):1978–1985.
- Bhugra C, Rambhatla S, Bakri A, Duddu SP, Miller DP, Pikal MJ, Lechuga-Ballesteros D. 2007. Prediction of the onset of crystallization of amorphous sucrose below the calorimetric glass transition temperature from correlations with mobility. *J Pharm Sci* 96(5):1258–1269.
- Telang C, Yu L, Suryanarayanan R. 2003. Effective inhibition of mannitol crystallization in frozen solutions by sodium chloride. *Pharm Res* 20(4):660–667.
- Kueltzo LA, Wang W, Randolph TW, Carpenter JF. 2008. Effects of solution conditions, processing parameters, and container materials on aggregation of a monoclonal antibody during freeze–thawing. *J Pharm Sci* 97(5):1801–1812.
- Izutsu KI, Hiyama Y, Yomota C, Kawanishi T. 2009. Near-infrared analysis of hydrogen-bonding in glass- and rubber-state amorphous saccharide solids. *AAPS PharmSciTech* 10(2):524–529.
- Sundaramurthi P, Suryanarayanan R. 2010. Influence of crystallizing and non-crystallizing cosolutes on trehalose crystallization during freeze-drying. *Pharm Res* 27:2384–2393.
- Izutsu KI, Yomota C, Aoyagi N. 2007. Inhibition of mannitol crystallization in frozen solutions by sodium phosphates and citrates. *Chem Pharm Bull* 55(4):565–570.

40. Brittain HG. 1999. Methods for the characterization of polymorphs. New York: Marcel Dekker, Inc., pp 227–278.
41. Rukiah M, Lefebvre J, Hernandez O, van Beek W, Serpelloni M. 2004. Ab initio structure determination of the gamma form of D-sorbitol (D-glucitol) by powder synchrotron X-ray diffraction. *J Appl Cryst* 37:766–772.
42. Connolly B, Patapoff TW, Wang YJ, Moore JM, Kamerzell TJ. 2009. Vibrational spectroscopy and chemometrics to characterize and quantify trehalose crystallization. *Anal Biochem* 399(1):48–57.
43. Tanaka H. 1999. Two-order-parameter description of liquids. I. A general model of glass transition covering its strong to fragile limit. *J Chem Phys* 111(7):3163–3174.
44. Tanaka H. 1999. Two-order-parameter description of liquids. II. Criteria for vitrification and predictions of our model. *J Chem Phys* 111(7):3175–3182.
45. Tanaka H. 2005. Relationship among glass-forming ability, fragility, and short-range bond ordering of liquids. *J Non-Cryst Solids* 351(8–9):678–690.
46. Tanaka H. 2005. Two-order-parameter model of the liquid-glass transition. III. Universal patterns of relaxations in glass-forming liquids. *J Non-Cryst Solids* 351(43–45):3396–3413.
47. Scopigno T, Ruocco G, Sette F, Monaco G. 2003. Is the fragility of a liquid embedded in the properties of its glass? *Science* 302(5646):849–852.